Soft elastomeric capacitors with an extended polymer matrix for strain sensing on concrete

Emmanuel Ogunniyi[a], Han Liu[b], Austin R.J. Downey[a,c], Simon Laflamme[b,d], Jian Li[e], Caroline Bennett[e], William Collins[e], Hongki Jo[f], and Paul Ziehl[a,c]

[a]Department of Mechanical Engineering, University of South Carolina, Columbia, USA
[b]Department of Civil, Construction and Environmental Engineering, Iowa State University, Iowa, USA
[c]Department of Civil and Environmental Engineering, University of South Carolina, Columbia, USA
[d]Department of Electrical and Computer Engineering, Iowa State University, Iowa, USA
[e]Department of Civil, Environmental and Architectural Engineering, The University of Kansas, Lawrence, USA
[f]Department of Civil, Architectural Engineering and Mechanics, The University of Arizona, Tucson, USA

ABSTRACT

Surface strain sensors, such as linear variable differential transformers, fiber Bragg gratings, and resistive strain gauges, have seen significant use for monitoring concrete infrastructure. However, spatial monitoring of concrete structures using these sensor systems is limited by challenges in the surface coverage provided by a specific sensor or issues related to mounting and maintaining numerous mechanical sensors on the structure. A potential solution to this challenge is the deployment of large-area electronics in the form of a sensing skin to provide complete coverage of a monitored area while being simple to apply and maintain. Along this line of effort, networks constituted of soft elastomeric capacitors have been deployed to monitor strain on steel and composite structures. However, using soft elastomeric capacitors on concrete surfaces has been challenging due to the electrical coupling between the sensors and concrete, which amplifies transduced strain signals obtained from the soft elastomeric capacitors. In this work, the authors investigate the isolation of the soft elastomeric capacitors from the concrete by extending the styrene-block-ethylene-co-butylene-block-styrene matrix of the soft elastomeric capacitors to include a decoupling layer between the electrode and the concrete. Experimental investigations are carried out on concrete specimens for which the soft elastomeric capacitor is adhered to with a thin layer of off-the-shelf epoxy and then loaded on the dynamic testing system to monitor strain provoked on the concrete samples. The results presented here demonstrate the viability of the electrically isolated soft elastomeric capacitors for monitoring strain on concrete structures. Initial comparisons between un-isolated and electrically isolated soft elastomeric capacitors showed that the nominal capacitance of the soft elastomeric capacitor is significantly lowered by adding an isolation layer of SEBS. Furthermore, strain results for the soft elastomeric capacitors are compared to ones from a resistive strain gauge and digital image correlation. The data obtained is significant for modifying soft elastomeric capacitors with the anticipation for future use on concrete structures.

Keywords: capacitive sensors, structural health monitoring, concrete strain, sensor isolation, sensing sheet, sensing skin

Further author information: (Send correspondence to Austin Downey)
Austin Downey: Email: austindowney@sc.edu

Sensors and Smart Structures Technologies for Civil, Mechanical, and Aerospace Systems 2023, edited by Zhongqing Su, Branko Glisic, Maria Pina Limongelli, Proc. of SPIE Vol. 12486, 1248618 · © 2023 SPIE · 0277-786X · doi: 10.1117/12.2658568

Downloaded From: https://www.spiedigitallibrary.org/conference-proceedings-of-spie on 23 Apr 2023
Terms of Use: https://www.spiedigitallibrary.org/terms-of-use

1. INTRODUCTION

Structural failures are primarily due to defective designs. However, several other factors have been identified that influence civil structure failures, such as faulty construction, foundation failure, extraordinary load, unexpected failure mode, and a combination of these causes.[1–3] While some of these causes are unavoidable, an excellent structural health monitoring (SHM) approach could prevent failures. The authors from references[4–6] expound on structural failures that result from precarious events, which lead to severe casualties, economic losses, and long-term risk for society. Therefore, understanding the behavior and performance of structures using effective structural health monitoring techniques is necessary to prevent these potential hazards.[7] Aside from public safety, researchers have demonstrated that SHM of civil structures has the potential to increase the life span of structures, lowers construction costs, enables early detection of risk, and improves the overall performance of the structure.[8,9]

Previous research efforts have investigated soft elastomeric capacitors for fatigue crack monitoring of steel. Soft elastomeric capacitors (SEC) have been used to monitor loads and fatigue cracks using the sensor's wireless network; the SECs are placed at strategic points on the bridge steel frame to monitor loading resulting from traffic.[10] Other investigations using the SEC also include monitoring damages such as cracks on bridge structures.[11] The authors have previously extended research efforts to monitor strain on concrete structures by adhering the SEC directly to the surface of the concrete. The investigations by Ogunniyi et. al.,[12] showed the need for electrical isolation of the concrete/sensor interface to prevent capacitive coupling between the SEC and the concrete; which leads to a capacitive signal that overestimates strain data. This is because concrete has innate capacitive properties while the SEC relies on capacitance measurements. The research demonstrated that using a rubber layer as an electrical isolation layer between the SEC and concrete is an effective way to reduce capacitive coupling.

Deploying the SEC with the use of additional isolation material is tasking, especially when installing multiple sensors. This work seeks to modify the SEC to achieve isolation by adding an extended polymer matrix of styrene-block-ethylene-co-butylene-block-styrene (SEBS) on both sides of the SEC sensor to act as an integrated isolation layer that extends the polymer matrix that makes up the SEC to five layers. The extended polymer matrix of SEBS is a transparent layer over the electrodes; this addition does not affect the sensor's sensitivity. With this design, a SEC is achieved for monitoring structural changes in concrete materials without needing separate isolation material.

This study evaluates the effectiveness of an extended polymer matrix on the SEC for measuring strains in concrete, building upon prior research in this area. In addition, the performance of the extended SEC is compared to that of commercially available resistive strain gauges and digital image correlation results. The contributions of this work are: 1) advancing previous research on strain sensing in concrete through the implementation of an extended polymer matrix of SEBS to minimize capacitance coupling between the SEC and concrete, and 2) conducting an experimental study on the capacitive coupling between a sensing skin and a concrete structure.

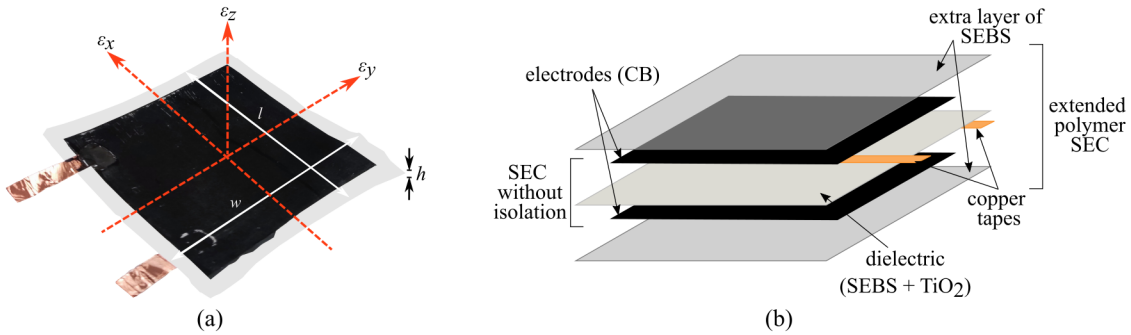

Figure 1. extended SEC where (a) shows the dry and ready-for-use sensor, and; (b) the schematic of the layers making up the extended sensor.

Downloaded From: https://www.spiedigitallibrary.org/conference-proceedings-of-spie on 23 Apr 2023
Terms of Use: https://www.spiedigitallibrary.org/terms-of-use

2. BACKGROUND STUDIES

This section describes the SEC sensor and its electromechanical modeling.

2.1 SEC Sensor

An SEC is composed of a dielectric layer sandwiched between two electrodes. The dielectric is made up of a SEBS matrix that has been filled with titania (TiO_2), which is an inorganic particle improving the permittivity and durability of the SEBS matrix.[13] The electrodes are made of the same organic matrix as the dielectric layer, but they are doped with carbon black (CB) particles to make a conductive polymer. With properties like ultraviolet light stabilization and antioxidant capabilities, these CB particles were chosen to improve conductivity at a low cost while extending the polymer's life.[14] In addition, the layers that make up the SEC have robust mechanical interlayer bonding since the electrodes, and the dielectric is made of the same SEBS polymer matrix.

Figure 1(a) depicts a single SEC with a surface area of 76.2 × 76.2 mm (3 × 3 in), whereas Figure 1(b) depicts a schematic of the sensor with an extended polymer matrix proposed by this work. It is worth noting that the geometry (such as form and size) can be changed. The resulting sensor has the following features: low cost, great ultra flexibility, mechanical robustness, ease of installation, and low power consumption required for sensing.

2.2 Electromechanical model

The SEC utilizes the deformation induced by external forces on its surface to measure strain. As the SEC deforms, its capacitance also changes in proportion to the deformation. This behavior allows the SEC to be modeled as a parallel plate capacitor, as expressed by the following equation.

$$C = e_0 e_r \frac{A}{h} \tag{1}$$

where $e_0 = 8.854\text{pF}/m$ denotes the vacuum permittivity, e_r is the dimensionless polymer relative permittivity, h represents the thickness of the dielectric layer, and $A = l \times w$ is the sensor area, with w and l being the width and length, respectively, as depicted in Figure 1(a). Assuming small changes in strains on the monitored surface, the differential change in capacitance ΔC can be obtained by differentiating Eq.(1).

$$\frac{\Delta C}{C_0} = \left(\frac{\Delta l}{l_0} + \frac{\Delta w}{w_0} - \frac{\Delta h}{h_0} \right) = \varepsilon_x + \varepsilon_y - \varepsilon_z \tag{2}$$

ΔC denotes the capacitance change of the SEC due to strain, and C_0 represents the initial value of the SEC capacitance. ε_x, ε_y and ε_z are the strain in the x, y and z respectively. The SEC is deployed in the $x - y$ for surface strain monitoring. Assuming plane stress and applying Hooke's law,

$$\varepsilon_z = -\frac{\nu}{1-\nu}(\varepsilon_x + \varepsilon_y) \tag{3}$$

By substituting Eq.(3) into Eq.(2), the capacitance response of a free-standing SEC can be obtained:

$$\frac{\Delta C}{C_0} = \frac{1}{1-\nu_0}(\varepsilon_x + \varepsilon_y) = \lambda_0(\varepsilon_x + \varepsilon_y) \tag{4}$$

where v_0 is the Poisson's ratio for the SEC, and λ_0 is the SEC's gauge factor

$$\frac{\Delta C}{C_0} = \lambda_0(\varepsilon_x + \varepsilon_y) \tag{5}$$

The gauge factor used in this paper is 1.7, which has been experimentally validated.[15]

$$\varepsilon_m = (\varepsilon_x + \varepsilon_y) \tag{6}$$

$$\frac{\Delta C}{C_0} = 1.7(\varepsilon_x + \varepsilon_y) \tag{7}$$

$$\frac{\Delta C}{1.7 C_0} = \varepsilon_m \tag{8}$$

where ε_m is the strain on the monitored surface.

Downloaded From: https://www.spiedigitallibrary.org/conference-proceedings-of-spie on 23 Apr 2023
Terms of Use: https://www.spiedigitallibrary.org/terms-of-use

3. METHODOLOGY

This section reports the fabrication procedure for the SEC with extended polymer matrix along with the experimental methodologies undertaken in this work.

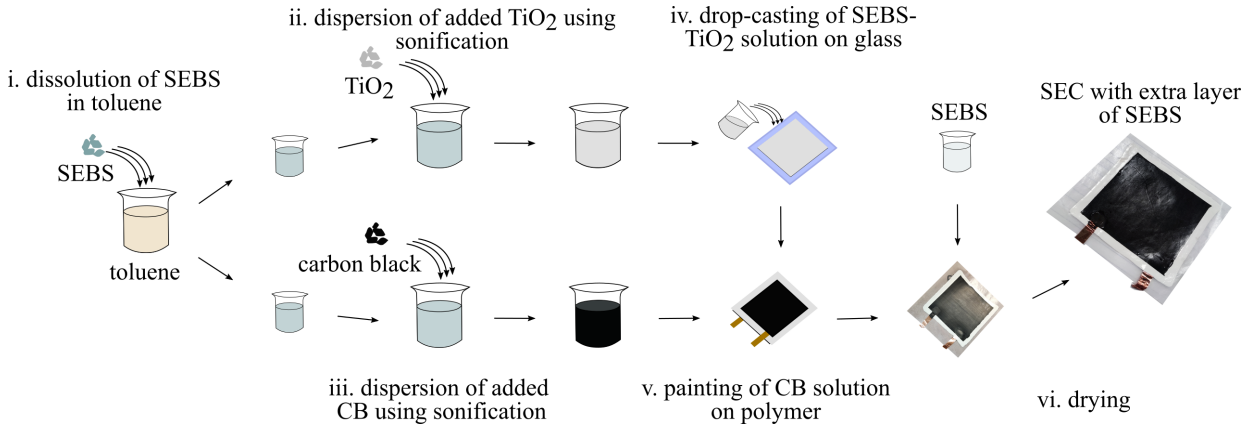

Figure 2. Extended SEC fabrication process.

3.1 Fabrication procedure for the SEC with extended polymer matrix

The process fabrication of the SEC with extended polymer matrix (Figure 1(b)) is described below, diagrammed in Figure 2, and broken down into the six steps that follow.

i. Toluene is used as the solvent to dissolve SEBS 500120M (Mediprene Dryex) particles to prepare the SEBS/toluene solution at a concentration of 160 g/L. PDMS-coated titania TiO_2 (-OSI$(CH_3)_2$-) rutile particles are dispersed in a portion of the SEBS/toluene solution at a concentration of 75 g/L.

ii. Titania particles are further uniformly dispersed in the SEBS matrix using an ultrasonic tip (Fisher Scientific D100 Sonic Dismembrator) at 20 kHz and 120 watts for 5 minutes.

iii. Another SEBS/toluene solution is prepared by dissolving SEBS 500050M in toluene for a concentration of 380 g/L. CB particles (Orion Printex XE 2-B) are scattered at a 25g/L concentration in the stock solution and dispersed using a low-speed homogenizer for one hour at 650 rpm.

iv. The dielectric layer is made utilizing a solution cast process, in which 20 ml of the prepared SEBS-TiO2 solution is dropped and cast directly onto a 76.2 × 76.2 mm (3 × 3 in) glass slide and covered for 24 hours in the fume hood to allow toluene to evaporate. The resulting film is peeled off from the glass plate and left to dry for 12 hours at room temperature.

v. The resulting SEBS-CB solution is brushed onto both the top and bottom surfaces of the dielectric, and a total of 4 layers of the conductive solution are brushed on each side with 30 minutes of drying between each layer. Two conductive copper tapes are implanted into the liquid electrode layers to provide mechanical connections for the wires that connect the sensor to the data acquisition system.

vi. The resulting multi-layer nanocomposite is allowed to dry for 24 hours. The SEC is then extended with an extra layer of nonconductive SEBS 500120M/toluene solution without TiO_2 on both surfaces for a composite configuration, preventing capacitive coupling between the electrode and the concrete layer.

Downloaded From: https://www.spiedigitallibrary.org/conference-proceedings-of-spie on 23 Apr 2023
Terms of Use: https://www.spiedigitallibrary.org/terms-of-use

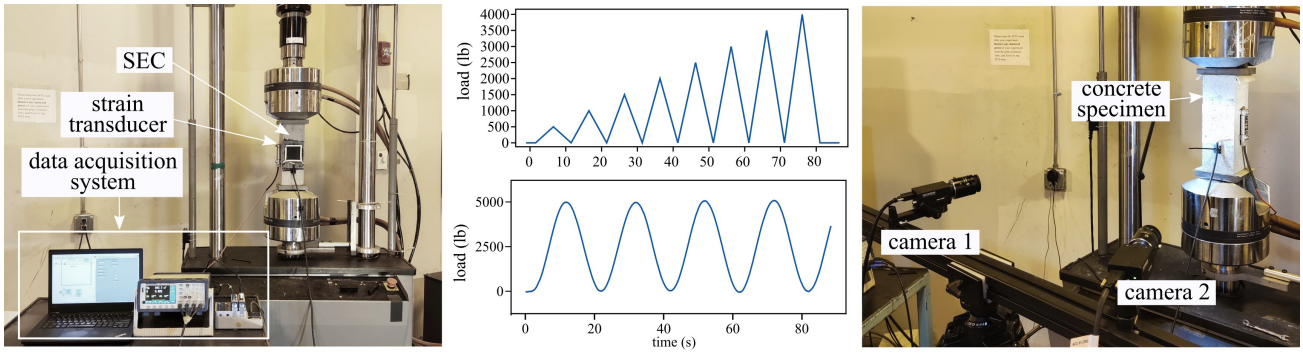

(a) (b) (c)

Figure 3. The specimen-scale testing experimental setup showing: (a) the concrete specimen on the dynamic testing system with the data acquisition system which includes the NI DAQ and BK Precision 891 300 kHz; (b) the loading procedure used in the experimental process, and; (c) DIC experimental setup for the strain data collection on the speckled concrete specimen.

3.2 Experimental Setup

Figure 3 illustrates the experimental setup employed in this study to examine the concrete samples. The concrete specimen is loaded using a dynamic testing device (MTS Model No. 609.25A-01) capable of supporting up to 250 kN of load, as shown in Figure 3(a).

The compressive tests were conducted on an unreinforced concrete specimen with dimensions of 0.305 × 0.102 × 0.102 m (4 × 4 × 12 in), manufactured using 3.5 L of water per 80 kg of a 27 MPa (4000 psi) strength concrete mix. The density of each sample was approximately 2014 kg/m3 (125.73 lb/ft3). To ensure reliable strain measurements, the surface of the concrete was scrubbed with sandpaper and cleaned thoroughly before the SEC was bonded to it using off-the-shelf bi-component epoxy. A stretch of about 2% of the initial dimension was applied to the SEC during installation to place it under initial strain, allowing it to deform along with the specimen during testing.

The performance of the SEC as a strain-sensing material on the concrete specimen was evaluated using a triangle and cyclic loading process, as illustrated in Figure 3(b). The loading was fixed-compression mode harmonic excitation at 0.05 Hz and ranged from 0 to 4000 lb. In addition, strain measurements on the concrete sample were collected under steady-state cyclic loading conditions using the SECs, strain transducer, and digital image correlation (DIC).

Capacitance values from the SEC were obtained by using an LCR meter (BK precision 891) with a drive frequency of 1 kHz and LabVIEW code to manage the data acquisition procedure. The collected capacitance values were then related to strain using the electromechanical model given in section 2. Data from a reusable surface-mount resistance bridge-based strain transducer (BDI ST350 model) was collected using a bridge analog input module (NI-9237 manufactured by NI), while load and displacement were acquired from the dynamic testing apparatus using an analog digitizer (NI-9239 manufactured by NI).

A DIC setup was employed to validate the strain on the surface of the SEC, as shown in Figure 3(c). The SEC was the image focus and area of interest for strain measurement, and image data from a 5 MP camera was analyzed using VIC-3D from Correlated Solutions.

Downloaded From: https://www.spiedigitallibrary.org/conference-proceedings-of-spie on 23 Apr 2023
Terms of Use: https://www.spiedigitallibrary.org/terms-of-use

4. RESULTS AND DISCUSSION

The following section presents an analysis of the findings from the study, including a discussion of the application and interpretations of the results.

4.1 Sensor nominal capacitance

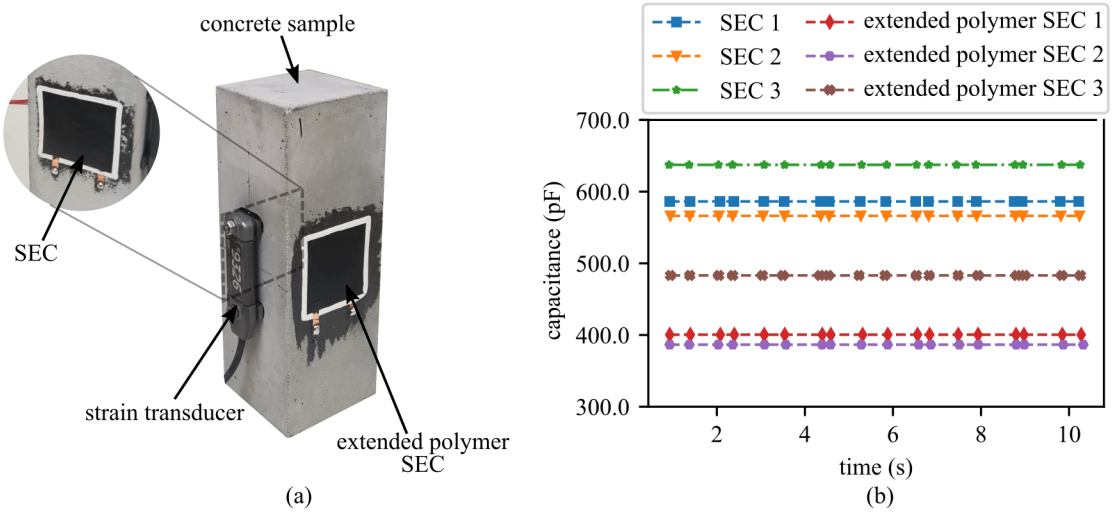

Figure 4. Shows (a) concrete specimen with SEC, extended layer SEC and strain transducer attached to it, and; (b) shows the nominal capacitance of the SECs upon adhering them to the concrete specimens.

The introduction of isolation on the SEC in the form of an extra layer of SEBS alters the nominal capacitance of the SEC. The extra layer of SEBS added to the SEC also increased the thickness of the sensor, therefore adding to the stiffness of the SEC. Increasing the SEC stiffness lowers its nominal capacitance. Figure 4(a) shows the SEC, extended layer SEC and strain transducer on the surface of the concrete, and Figure 4(b) shows the nominal capacitance of both SEC upon adhering them to the concrete surface. For the six SECs sample observed, the SECs without an extra layer of SEBS have higher nominal capacitance compared to ones with an extra layer of SEBS.

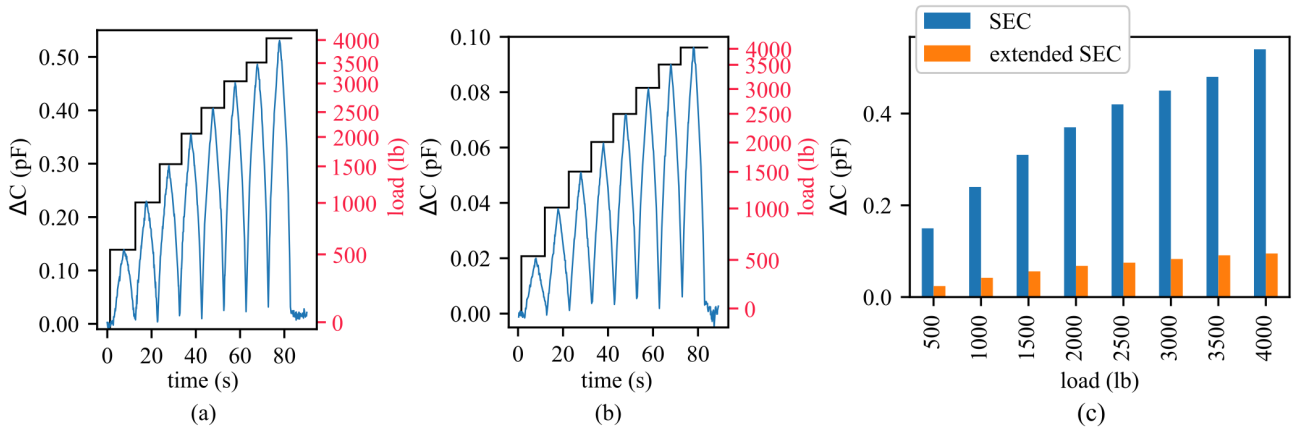

Figure 5. Capacitance change in response to load observed using (a) SEC; (b) extended SEC, and; (c) both sensors.

Downloaded From: https://www.spiedigitallibrary.org/conference-proceedings-of-spie on 23 Apr 2023
Terms of Use: https://www.spiedigitallibrary.org/terms-of-use

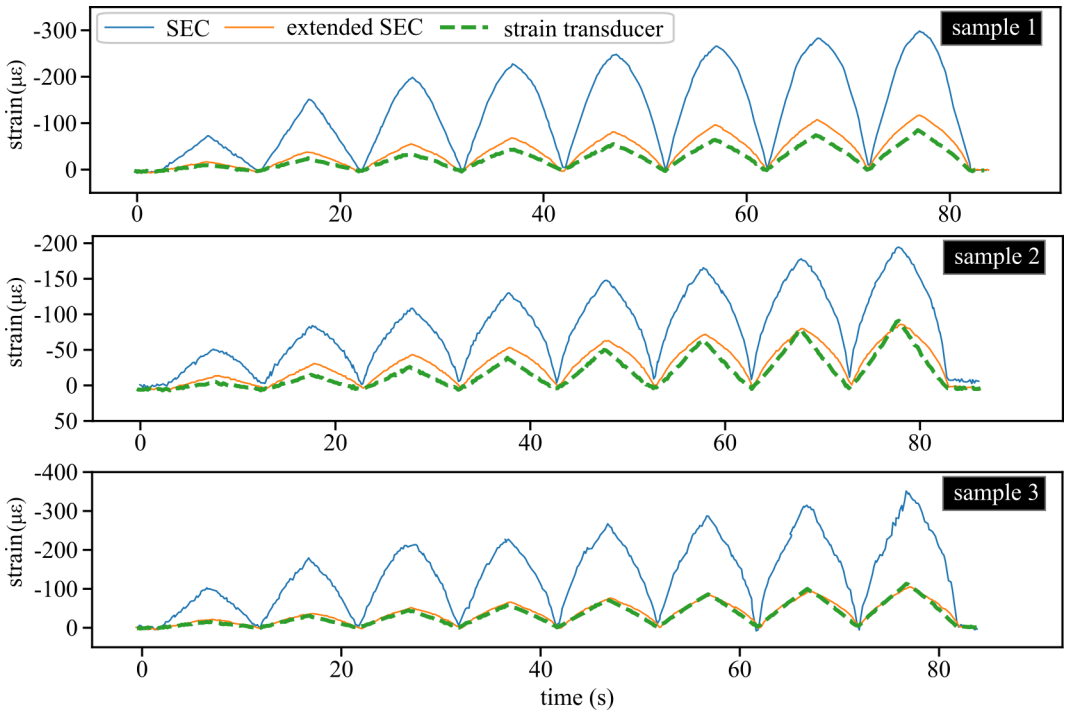

Figure 6. Strain measured from three concrete specimens using SEC, extended SEC, and strain transducer.

4.1.1 Responses to loading

The SECs were subjected to increasing triangle loading as shown in fig 3(b), and capacitance change to load in both SEC is shown in Figure 5(a) and (b). As seen in both sensors' responses to load, the capacitance change decreases as the incremental load increases from 500 to 4000 lb at an increment of 500 lb. Figure 5(a) shows the response of the SEC to incremental load. The first 500 lb load increment causes a 0.14 pF change in the nominal capacitance of the SEC. However, compared to Figure 5(b), which is the capacitance change for the extended SEC, the first 500 lb load addition resulted in a 0.02 pF change in capacitance. The subsequent addition of a 500 lb load measured by both sensors showed a similar trend. Equal load resulted in a bigger capacitance change in the SEC compared to the extended SEC as shown in the barplot of Figure 5(c). Adding an extra layer of SEBS to the SEC greatly reduces the capacitive coupling that results an overestimated measurement in the SEC.

4.2 Strain results

Strain data were acquired from three concrete specimens subjected to compressive loads using an SEC, an extended SEC, and a strain transducer. Figure 6 display the strain obtained from the three samples. As observed in the three samples, the strain measured by the SEC is higher than the other two sensors, and the strain from the extended SEC closely agrees with the one measured by the strain transducer. Therefore, the strain measured by the SEC is overestimated compared to the actual strain in the concrete specimen; as discussed in detail in reference.[12]

The strain on the SEC's surface bonded to the concrete was examined using digital image correlation for one sensor. The concrete specimen was loaded using the described cyclic loading method as part of the DIC investigation utilizing the experimental setup indicated in Figure 3(c). The strain map for the first 6.03 s of Figure 7(a) is shown in Figure 7(b) at an interval of 0.6 s. The DIC strain data displays the distributed strain along the y-axis (ε_y)) on the surface of the SEC. Maximum strain is observed at 3.03 s where the DIC recorded a strain of -82 $\mu\varepsilon$, the SEC measured a strain of -376 $\mu\varepsilon$, while the extended SEC measured a strain of -112 $\mu\varepsilon$. This data confirms that the strains measured by the extended SEC and DIC are close, while the SEC overreports the strain.

Downloaded From: https://www.spiedigitallibrary.org/conference-proceedings-of-spie on 23 Apr 2023
Terms of Use: https://www.spiedigitallibrary.org/terms-of-use

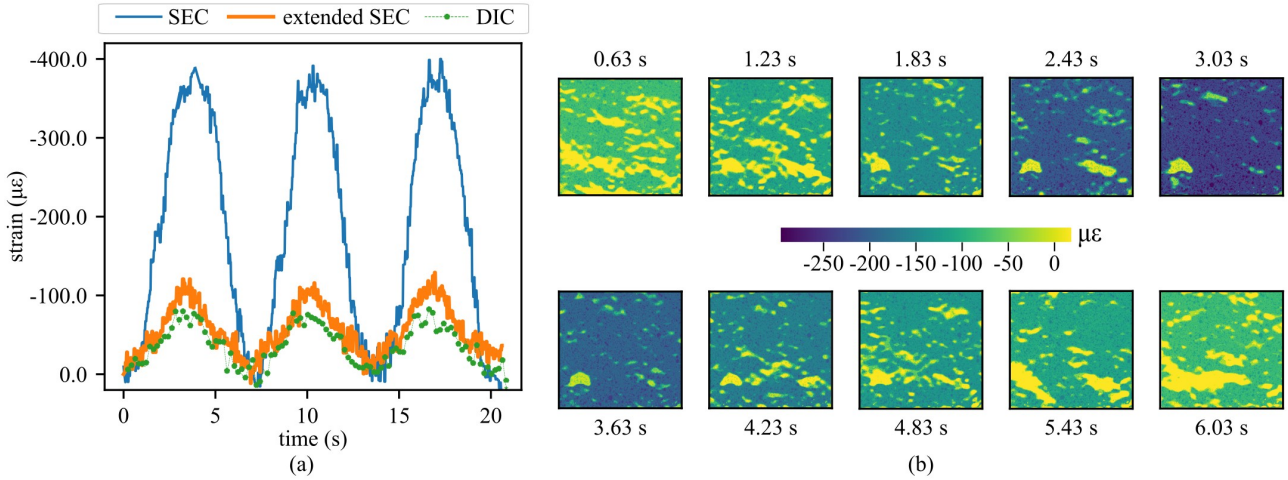

Figure 7. Detailed DIC investigation for strain data obtained from a sensor, showing: (a) data obtained from an SEC, extended SEC, and digital image correlation, and; (b) strain map from the digital image correlation from 0.63 s to 6.03 s at an interval of 0.6 s.

5. CONCLUSION

This study investigated using an extended soft elastomeric capacitor (SEC with an extra layer of SEBS) on concrete. This extra layer was added to minimize the capacitive coupling between the SEC and concrete, which results in overestimated measurements, as observed in previous research efforts. The paper observed the response to loading for the SEC and the extended SEC by comparing the relative capacitance change in both sensors under the same load. This investigation shows that the SEC without extra layers of SEBS has a higher capacitance change for each change in loading than the SEC with extra layers of SEBS.

Strain data obtained from the capacitance change in both SECs and the off-the-shelf strain transducer showed that the strain data from the extended SEC and strain transducer are more closely aligned. Further validation of strain data was carried out using digital image correlation, which also showed that the extended SEC is viable for strain measurements on concrete structures. The investigations report improvement in strain data from the SEC when used on concrete surfaces, and future research will focus on applications for measurements on concrete structures.

ACKNOWLEDGMENTS

The authors gratefully acknowledge the financial support of the Departments of Transportation of Iowa, Kansas, South Carolina, and North Carolina, through the Transportation Pooled Fund Study TPF-5(449).

REFERENCES

[1] Almarwae, M., "Structural failure of buildings: Issues and challenges," *World Scientific News* (66), 97–108 (2017).

[2] Gakkai, D., "Bridge collapses around the world: Causes and mechanisms," *Proceedings of the IABSE-JSCE Joint Conference on Advances in Bridge Engineering-III, August 21-22, 2015, Dhaka, Bangladesh* , 651.

[3] Chandra, S., "Bridge failure and consequences," **7**, JETIR (2020).

[4] Song, G., Wang, C., and Wang, B., "Structural health monitoring (shm) of civil structures," *Applied Sciences (Switzerland)* **7** (8 2017).

[5] LJ Bikoko, T. G., Tchamba, J. C., and Ndubisi Okonta, F., "A comprehensive review of failure and collapse of buildings/structures," *International Journal of Civil Engineering and Technology* **10**(3) (2019).

[6] Wardhana, K., Hadipriono, F. C., and Asce, F., "Analysis of recent bridge failures in the united states,"

Downloaded From: https://www.spiedigitallibrary.org/conference-proceedings-of-spie on 23 Apr 2023
Terms of Use: https://www.spiedigitallibrary.org/terms-of-use

[7] Ozer, E. and Feng, M. Q., "Structural health monitoring," *Start-Up Creation* , 345–367, Elsevier (2020).
[8] Alokita, S., Rahul, V., Jayakrishna, K., Kar, V., Rajesh, M., Thirumalini, S., and Manikandan, M., "Recent advances and trends in structural health monitoring," in [*Structural health monitoring of biocomposites, fibre-reinforced composites and hybrid composites*], 53–73, Elsevier (2019).
[9] Omenzetter, P., Yazgan, U., Soyoz, S., and Limongelli, M. P., "Quantifying the value of shm for emergency management of bridges at-risk from seismic damage," in [*Joint COST Actions TU1402 & TU1406 and IABSE WC1 Workshop: Quantifying the Value of Structural Health Monitoring for the Reliable Bridge Management*], 4–5 (2017).
[10] Taher, S. A., Li, J., Jeong, J.-H., Laflamme, S., Jo, H., Bennett, C., Collins, W. N., and Downey, A. R. J., "Structural health monitoring of fatigue cracks for steel bridges with wireless large-area strain sensors," *Sensors* **22**, 5076 (jul 2022).
[11] Yan, J., Downey, A., Cancelli, A., Laflamme, S., Chen, A., Li, J., and Ubertini, F., "Concrete crack detection and monitoring using a capacitive dense sensor array," *Sensors (Switzerland)* **19** (4 2019).
[12] Ogunniyi, E., Vereen, A., Downey, A., Laflamme, S., Li, J., Bennett, C. R., Collins, W., Jo, H., Henderson, A., and Ziehl, P., "Investigation of electrically isolated capacitive sensing skins on concrete to reduce structure/sensor capacitive coupling," *Measurement Science and Technology* (2023).
[13] Stoyanov, H., Kollosche, M., McCarthy, D. N., and Kofod, G., "Molecular composites with enhanced energy density for electroactive polymers," *Journal of Materials Chemistry* **20**(35), 7558–7564 (2010).
[14] Huang, J. C., "Carbon black filled conducting polymers and polymer blends," *Advances in Polymer Technology* **21**, 299–313 (12 2002).
[15] Liu, H., Laflamme, S., Li, J., Bennett, C., Collins, W., Downey, A., Ziehl, P., and Jo, H., "Investigation of surface textured sensing skin for fatigue crack localization and quantification," *Smart Materials and Structures* **30** (10 2021).

Downloaded From: https://www.spiedigitallibrary.org/conference-proceedings-of-spie on 23 Apr 2023
Terms of Use: https://www.spiedigitallibrary.org/terms-of-use